

<https://doi.org/10.33472/AFJBS.6.2.2024.412-424>



African Journal of Biological Sciences



Research Paper

Open Access

Role of Tissue Doppler Echocardiogram and Insulin Like Growth Factor Binding Protein Type 2 in Diagnosis and Evaluation of Severity of Pediatric Pulmonary Hypertension

Somaia Abdelsamie Elwan¹, Amira Osama Abdel Ghafar², Lamiaa Ragab El Deep³, Eman Gamal Abdelrahman¹

¹ Pediatric Department, Benha University, Benha, Egypt

² Clinical pathology Department, Benha University, Benha, Egypt

³ Pediatric Department, Metobas Hospital, Egypt

somaiaelwan@gmail.com, amera.osama@fmed.bu.edu.eg, lamiaa.5572@gmail.com, egaabfm@gmail.com

Article History

Volume 6, Issue 2, April 2024

Received: 19 April 2024

Accepted: 2 May 2024

Published: 16 May 2024

doi: 10.33472/AFJBS.6.2.2024.412-424

Abstract: Objective: To evaluate the role of tissue Doppler echocardiogram and insulin like growth factor binding protein type 2 in diagnosis and evaluation of severity of pediatric pulmonary hypertension.

Methods: This cross-sectional case, control study included 80 children divide into two equal groups: Group (A): patients with PHT diagnosed by Echocardiogram as mean pulmonary artery pressure more than 25 mmHg (MPAP>25). Group (B): age and sex matched to healthy patients . Detailed clinical assessments, tissue Doppler echocardiographic examinations, and IGFBP-2 measurements using ELISA were conducted.

Results: There is RV dilataion and disfunction (higher MPI) more in cases group .

ROC analysis revealed a significant excellent AUC of 0.923 for IGFBP2 with a 95% CI = 0.862 – 0.984 (P < 0.001). The best cutoff point was >168 mg\L, at which sensitivity and specificity were 95% and 77.5%, respectively for prediction of PH. IGFBP2 showed significant positive correlations with MPI of RV (r = 0.619, P < 0.001).

Conclusion: PHT was associated with RV dilatation and dysfunction wither systolic, and diastolic cmfirmed by high MPI of RV. IGFBP2 is an excellent predictor of PH which sensitivity and specificity were 95% and 77.5%, respectively IGFBP2 is positively associated with severity of PH showed significant positive correlations with conventional echocardiographic and tissue doppler parameters.

Keywords: Tissue Doppler Echocardiogram, IGFBP-2, Pediatric Pulmonary Hypertension, Disease Severity

Introduction: Pulmonary arterial hypertension (PAH) is a grave condition marked by heightened remodeling of the pulmonary vasculature and increased mean pulmonary artery pressures. This condition exhibits significant heterogeneity and has been categorized into

five distinct clinical subgroups by the Sixth WSPH in 2019. Despite an incomplete understanding of its exact underlying mechanisms, the increase in pulmonary vascular resistance and the consequent development of right heart failure are universal features in all individuals suffering from PAH (1).

Over the past fifty years, the array of therapeutic modalities available for PAH has significantly broadened, leading to enhanced functional capacity and hemodynamic outcomes in affected individuals. PAH manifests insidiously, featuring nonspecific initial symptoms, often necessitating diagnostic confirmation through cardiac catheterization (2). The analysis of the frequently utilized blood biomarker NTproBNP, which serves as a marker for cardiac dysfunction and heightened myocardial stretch, is rendered intricate due to the presence of various confounding variables, including renal function and left heart disease. There is a pressing need for a biomarker that is more specific to pulmonary vascular pathology, precise in its measurements, and directly linked to disease causality. Such a biomarker would not only enhance non-invasive diagnostic capabilities but also deepen our comprehension of pathobiological mechanisms and improve the noninvasive monitoring of disease advancement (3).

IGF axis comprises a duo of hormones (IGF1 and IGF2), which interact with two distinct receptors (IGFR1 and IGFR2), along with six binding proteins (IGFBP1-6) characterized by their strong affinity for IGFs. In the typical scenario, IGFs within the bloodstream tend to form complexes with specific binding proteins, thereby establishing a reservoir of IGFs that is shielded from degradation processes. However, it is noteworthy that IGFBPs also exert direct effects on cellular function through mechanisms independent of IGFs. Of particular interest, IGFBP2 may hold a specific relevance to lung function, as evidenced by a strong correlation between circulating levels of IGFBP2 and the progression of pulmonary fibrosis, as well as its treatment (4).

Due to the intricate morphology and myocardial structure of the RV, along with its reliance on loading conditions, the accurate echocardiographic evaluation of RV function using traditional volumetric parameters like EF presents a considerable challenge. In contrast, CMR imaging offers a broader field of view and lacks restrictions related to specific anatomical planes, potentially mitigating some of these challenges (5).

Nevertheless, the utilization of CMR imaging in young children necessitates the administration of general anesthesia or profound sedation, thereby limiting its applicability in this population. As a substitute, echocardiographic assessments of longitudinal contractility, like the determination of DTI evaluations of septal and annular basal myocardial segments or TAPSE through M-mode echocardiography, present feasible alternatives. These methodologies may offer particular advantages in the assessment of RV systolic function. Unlike the left ventricle, which expels a significant proportion of its stroke volume through torsional modifications in geometry, the stroke volume of the RV is predominantly contingent upon longitudinal contraction (6).

Therefore, the purpose of this study is to evaluate the role of tissue Doppler echocardiogram and IGFBP-2 in diagnosis and evaluation of severity of pediatric pulmonary hypertension.

Patients and Methods

This cross-sectional case, control study was conducted in Pediatric cardiology Department, Benha University Hospitals, Benha, Egypt in period of 12 months starting from May-2022 to May-2023.

The study was approved by the Ethics Committee of Faculty of Medicine, Benha University, Egypt and informed written or oral consent was taken from patient's relatives .

Inclusion criteria were age from Birth to 16 years, both genders and patients with Pulmonary hypertension both congenital and acquired cases .

Exclusion criteria were diabetes mellitus, malignancy, obesity, chronic kidney disease and normal pulmonary pressure.

This study included 80 children divide into two equal groups: Group (A): patients with PHT Diagnosed by Echocardiogram (MPAP>25mmHg). Group (B): sex and age matched to healthy patient group.

All patients were subjected to:

Full history taking from subjects or their relatives including patient's full name, age, sex, height, weight, BMI. General examination, cardiac examination, chest examination , abdominal examination , and neurological examination

Cardiovascular measurements:

All cardiograms were operated by an efficient pediatric cardiologist using transthoracic two-dimensional M-mode and Doppler echocardiography by using Philips Affiniti 50c. we used transducers 3S and 6S, 2D mode, M mode, Color Doppler, Color Power continuous Doppler, Pulse wave Doppler , Auto color and auto Doppler. Transport mode: (7).

Echocardiography measurements were:

Systolic pulmonary artery pressure:

SPAP can be approximated using the peak TR velocity measured via continuous-wave Doppler, applying the modified Bernoulli equation, provided there is no obstruction in the RVOT. This approach stands as the most effective non-invasive means of estimating SPAP. To ascertain the RVSP, the result of the Bernoulli equation must be supplemented with the mean RA pressure. In the context where there is no obstruction in the RVOT, the SPAP is considered equivalent to the RVSP. The ensuing formula is delineated as follows:

$$RVSP = SPAP = 4(TR \max)^2 + mRAP \quad (9).$$

Diastolic pulmonary artery pressure estimation may be achieved through the assessment of peak and end-diastolic velocities of the pulmonary regurgitation jet (10).

$$DPAP = PR \text{ end diastolic pressure gradient} + \text{Right Atrial Pressure}$$

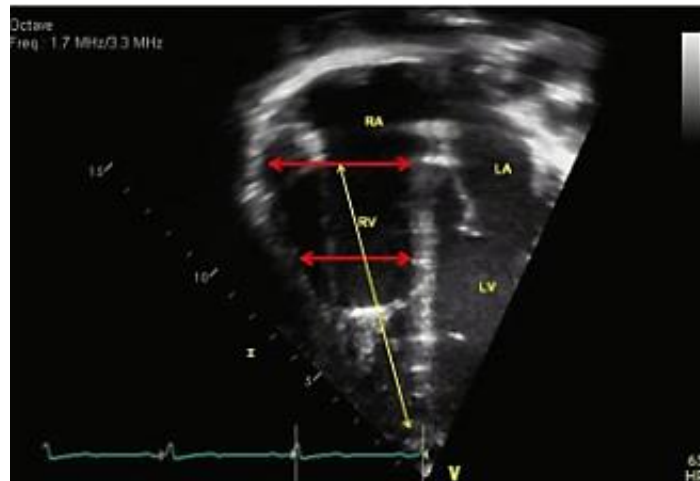
Mean Pulmonary artery pressure:

Can be estimated by Bernoulli equation. $MPAP = 2\sqrt{3} \text{rd of PADP} + 1\sqrt{3} \text{rd of PASP}$.

Pulmonary acceleration time is calculated as the time interval from the onset of systolic flow to the peak velocity (11).

The right ventricular dimensions

The right ventricular dimensions are obtained using conventional echocardiography. The linear measurements include: basal RV diameter, mid RV diameter and RV out tract flow diameter. In the apical four-chamber view, the basal diameter is gauged at the tricuspid valve level, while the mid- RV diameter is assessed at the midportion of the RV, specifically at the level of the papillary muscle of the LV. The RVOT diameter is measured in the short-axis parasternal view (12).



Determination of the dimensions of the right ventricle at the end of diastole, focusing on the basal dimension at the level of the tricuspid valve, as well as the outflow tract dimension (indicated by red arrows).

Right ventricular systolic Function (TAPSE): We had assessed RV function by evaluating TAPSE which measured by M-mode echocardiography. It quantifies the longitudinal excursion of the tricuspid annulus over the course of systole. The measurement is taken as the peak excursion of the tricuspid annulus towards the apex during ventricular systole (13)

Right ventricular diastolic Function E/A ratio Deceleration time: These parameters are typically obtained from the tricuspid inflow using Doppler echocardiography. the E/A ratio (early to late diastolic filling velocity) and deceleration time of the E wave reflect the diastolic function of the RV (14).

Tissue Doppler Imaging (TDI) is a sophisticated modality used to assess myocardial velocities by strategically positioning the sample volume within specific myocardial segments. This method allows for the precise measurement of velocities across various phases of the cardiac cycle, encompassing the S wave for systolic velocity, the E wave for early diastolic velocity, and the A wave for late diastolic velocity (15).

Within the apical 4-chamber view, the utilization of TDI was directed towards the assessment of RV's free wall. In order to attain an optimal operational state, a Nyquist limit ranging from 15 to 20 cm/s was imposed, while the sweep speed was meticulously set between 50 and 100 mm/s to amplify the resolution of myocardial velocities.

Myocardial performance index on right ventricle by tissue doppler

MPI, colloquially referred to as the Tei index, stands as a pivotal quantitative gauge that intricately appraises the myocardium's functional efficacy by adeptly encapsulating evaluations of both systolic and diastolic functionalities. For the RV, the formula is adapted accordingly (16):

$$MPI_{RV} = (ICT + IRT) / ET$$

When MPI_{RV}: Myocardial Performance Index for the right ventricle, ICT: Isovolumetric contraction time (time from the end of the S wave to the beginning of the E wave), IRT: Isovolumetric relaxation time (time from the end of the E wave to the beginning of the A wave) and ET: Ejection time (time from the beginning to the end of the ejection phase).

Measurements of IGFBP-2 by ELISA.

Aseptically, a volume of five millimeters of venous blood was extracted from each participant and placed into non-anticoagulant-containing plain tubes. Subsequently, the samples were maintained at ambient temperature to facilitate the formation of blood clots before being centrifuged at 2000 RPM for a duration of 5 minutes. The resultant serum is stored at -80 °C until analysis. Serum ILGBP2 level is measured by ELISA. All methods were performed according to the manufacturer's instructions.

Statistical analysis

Data management and statistical analysis were done using SPSS version 28 (IBM, Armonk, New York, United States). Quantitative data were succinctly represented by means coupled with standard deviations or medians flanked by ranges. Categorical data were rendered as numerical counts juxtaposed with corresponding percentages. The comparison of quantitative data across the studied groups was achieved through the application of statistical tests, specifically the independent t-test for normally distributed variables and the Mann-Whitney U test for those that deviated from normality. Categorical data, on the other hand, were compared utilizing either the Chi-square or Fisher's exact test. ROC analysis was performed to assess the diagnostic utility of IGFBP2 in identifying pulmonary hypertension. Correlation analyses were conducted employing Pearson's or Spearman's correlation coefficients. Furthermore, a multivariate linear regression analysis was executed to forecast IGFBP2 levels. Additionally, multivariate logistic regression analysis was done to predict pulmonary hypertension. P values less than 0.05 were considered significant.

Results

Table 1: General characteristics of the studied groups, and Etiology of pulmonary hypertension

		Group A (n = 40)	Group B (n = 40)	P value
Age				
Neonates		6 (15)	7 (17.5)	0.503
1 m - 2 y		15 (37.5)	9 (22.5)	
2 y - 6 y		9 (22.5)	13 (32.5)	
> 6 y		10 (25)	11 (27.5)	
Sex	Males	29 (72.5)	29 (72.5)	1.0
	Females	11 (27.5)	11 (27.5)	
Residence	Urban	18 (45)	18 (45)	1.0
	Rural	22 (55)	22 (55)	
Etiology of pulmonary hypertension				
(PAH) included (congenital Defects, persistent pulmonary hypertension of newborn, And idiopathic PAH)			17 (42.5)	
Left heart disease included (Mitral valve lesion, Heart failure)			13 (32.5)	
Upper airway and Chest disease			10 (25)	

Data are presented as frequency (%), PAH: Pulmonary arterial hypertension, No substantially significant differences were observed between the studied groups regarding age ($P = 0.503$), sex ($P = 1.0$), and residence ($P = 1.0$).

Table 1: Echo parameters, IGFBP2 level in the studied groups

	Group A (n = 40)	Group B (n = 40)	P-value
I Conventional parameters			
<i>Pulmonary parameters</i>			
MPAP (mmHg)	63 ±17	21 ±3	<0.001*
PAAT (ms)	92.1 ±26.1	72.2 ±14.1	<0.001*
<i>RV diameters</i>			
basal (cm)	2.6 ±0.8	1.9 ±0.4	<0.001*
Mid RV (cm)	1.8 ±0.5	1.3 ±0.2	<0.001*
RV out tract (cm)	2.5 (1.1 - 6.2)	1.6 (1.1 - 5.9)	<0.001*
<i>TAPSE</i>			
TAPSE on RV (cm)	13.1 ±1.5	16.7 ±3.4	<0.001*
<i>E/A on RV</i>			
E wave (cm/s)	86.3 ±15.6	81.9 ±17.2	0.229
A wave (cm/s)	51.7 ±9.2	35.6 ±9.8	<0.001*
E/A (cm/s)	1.7 ±0.4	2.3 ±0.3	<0.001*
DT (ms)	126.8 ±32.1	117.8 ±18.9	0.132
IGFBP2 (ng/ml)	260 ±75	144 ±37	<0.001*

Data are presented as Mean ±SD, Median (min-max), PAAT: Pulmonary Artery Acceleration Time; SPAP: Systolic Pulmonary Artery Pressure; dPAD: Diastolic Pulmonary Artery Pressure; TAPSE: Tricuspid Annular Plane Systolic Excursion; DT: Deceleration Time, * Significant P-value; IGFBP2: Insulin-like Growth Factor Binding Protein 2.

Group A revealed significantly higher MPAP, PAAT and IGFBP2 than group B. Group A revealed significantly higher Basal, Mid RV, and RV out tract diameters than group B ($P < 0.001$). Group B showed significantly higher TAPSE than Group A (16.7 ± 3.4 vs. 13.1 ± 1.5 , $P < 0.001$). Group A demonstrated a significantly higher A wave (51.7 ± 9.2 vs. 35.6 ± 9.8 , $P < 0.001$) than Group B. In contrast, they demonstrated significantly lower E/A (1.7 ± 0.4 vs. 2.3 ± 0.3 , $P < 0.001$). No significant differences were observed regarding E wave and DT ($P = 0.229$ and 0.132 , respectively).

ROC analysis of IGFBP2 to diagnose pulmonary hypertension

ROC analysis was done for IGFBP2 to predict pulmonary hypertension. It revealed a significant excellent AUC of 0.923, with a 95% CI = 0.862 – 0.984 ($P < 0.001$). The best cutoff point was >168 Mg \L , at which sensitivity and specificity were 95% and 77.5%, respectively. The negative and positive predictive values were 93.9% and 80.9%, in respective manner. **(Figure 1)**

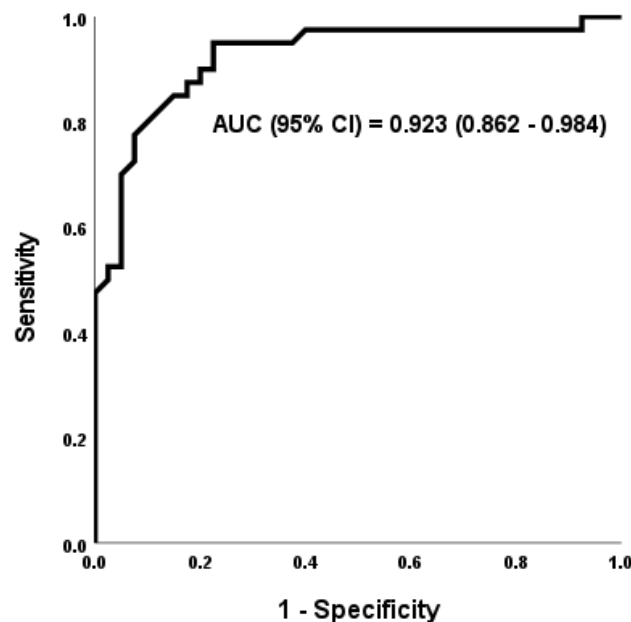


Figure 1: ROC analysis of IGFBP2 to diagnose pulmonary hypertension

Table 2: Statistical Correlation of echo parameters and tissue Doppler parameters with IGFBP2

	IGFBP2 (ng/ml)	
	r	P
<i>Pulmonary parameters</i>		
MPAP	.949	<.001*
PAAT	-.446	0.004*
<i>RV diameters</i>		
Basal (cm)	.597	<.001*
Mid RV (cm)	.494	0.001*
RV out tract (cm)	0.187	0.247
<i>TAPSE</i>		
TAPSE on RV	-0.074	0.648
<i>E/A on RV</i>		
E wave (cm/s)	.630	<.001*
A wave (cm/s)	0.118	0.468
E/A (cm/s)	.452	0.003*
DT (ms)	0.053	0.747
<i>TDI on RV</i>		
S wave (cm/s)	0.155	0.340
E wave (cm/s)	.487	0.001*
A wave (cm/s)	.384	0.014*
ICT (m/s)	0.015	0.927
IRT (m/s)	0.005	0.975
ET (m/s)	-.545	<.001*
MPI	.619	<.001*

* Significant P-value; mPAP: Mean Pulmonary Artery Pressure; PAAT: Pulmonary Artery Acceleration Time; TAPSE: Tricuspid Annular Plane Systolic Excursion; DT: Deceleration Time.

IGFBP2 showed significant positive correlations with MPAP ($r = 0.949$, $P < 0.001$), and PAAT ($r = -0.446$, $P = 0.004$). IGFBP2 showed significant positive correlations with the Basal diameter ($r = 0.597$, $P < 0.001$) and Mid RV parameters ($r = 0.494$, $P = 0.001$). No significant correlation was reported with the RV out tract diameter ($P = 0.247$). IGFBP2 showed significant positive correlations with E wave ($r = 0.630$, $P < 0.001$) and E/A ($r = 0.452$, $P = 0.003$). No significant correlations were reported with A wave ($P = 0.468$) and DT ($P = 0.747$). IGFBP2 showed significant positive correlations with MPI ($r = 0.619$, $P < 0.001$).

Table 4: Multivariate linear regression analysis to predict IGFBP2, Multivariate logistic regression analysis to predict pulmonary hypertension.

	B (95% CI)[†]	P-value
<i>Pulmonary parameters</i>		
SPAP	4.091 (3.539 - 4.644)	<.001*
dPAP	5.828 (2.277 - 9.38)	0.002*
PAAT	-0.888 (-1.766 - -0.011)	0.047*
<i>RV diameters</i>		
Proximal (cm)	46.329 (21.387 - 71.272)	<.001*
Distal (cm)	54.261 (6.68 - 101.842)	0.027*
<i>E/A on RV</i>		
E wave (cm/s)	2.514 (1.351 - 3.677)	<.001*
E/A (cm/s)	75.205 (20.031 - 130.379)	0.009*
<i>TDI on RV</i>		
E wave (cm/s)	10.343 (3.216 - 17.47)	0.006*
A wave (cm/s)	5.202 (-0.13 - 10.535)	0.056
ET (m/s)	-0.641 (-1.16 - -0.121)	0.017*
MPI	736.669 (293.542 - 1179.796)	0.002*
	OR (95% CI) †	P-value
<i>Pulmonary parameters</i>		
PAAT	1.05 (1.024 - 1.077)	<0.001*
<i>RV diameters</i>		
Proximal diameter (cm)	9.109 (3.116 - 26.635)	<0.001*
Distal diameter (cm)	59.645 (10.077 - 353.035)	<0.001*
Peripheral diameter (cm)	2.117 (1.296 - 3.459)	0.003*
<i>TAPSE</i>		
TAPSE on RV	2.214 (1.548 - 3.166)	<0.001*
<i>E/A on RV</i>		
A wave (cm/s)	1.202 (1.109 - 1.303)	<0.001*
E/A (cm/s)	0.002 (0 - 0.033)	<0.001*
<i>TDI on RV</i>		
S wave (cm/s)	0.732 (0.607 - 0.883)	0.001*
A wave (cm/s)	1.393 (1.176 - 1.65)	<0.001*
ET (m/s)	0.981 (0.968 - 0.995)	0.007*
MPI	9.924x10 ¹⁶ (4.380x10 ⁸ - 2.248x10 ²⁵)	<0.001*
<i>Biological marker</i>		
IGFBP2 (ng/ml)	1.039 (1.021 - 1.058)	<0.001*

*Significant P-value; †Adjusted for age, gender, and residence; B: regression coefficient; 95% CI: 95% Confidence interval; dPAD: Diastolic Pulmonary Artery Pressure; PAAT: Pulmonary Artery Acceleration Time; SPAP: Systolic Pulmonary Artery Pressure; ICT: Isovolumic Contraction Time; ET: Ejection Time; IRT: Isovolumic Relaxation Time; MPI: Myocardial Performance Index.

Multivariate linear regression analysis was used to predict IGFBP2. All significant variables on the univariate level were included in multivariate models, adjusted for age, gender, and residence. Regarding pulmonary parameters, the predictors were SPAP (B = 4.091, 95% CI = 3.539 - 4.644, P = <.001), dPAP (5.828, 95% CI = 2.277 - 9.38, P = 0.002), and PAAT (-0.888,

95% CI = -1.766 - -0.011, P = 0.047). Regarding RV diameters, proximal (B = 46.329, 95% CI = 21.387 - 71.272, P = <.001) and distal (54.261, 95% CI = 6.68 - 101.842, P = 0.027) diameters were significant predictors. Regarding E/A on RV, E wave (B = 2.514, 95% CI = 1.351 - 3.677, P = <.001) and E/A (B = 75.205, 95% CI = 20.031 - 130.379, P = 0.009) were significant predictors. Regarding TDI on RV, MPI (B = 736.669, 95% CI = 293.542 - 1179.796, P = 0.002) was a significant predictor, in addition to E wave (B = 10.343, 95% CI = 3.216 - 17.47, P = 0.006) and ET (B = -0.641, 95% CI = -1.16 - -0.121, P = 0.017). Multivariate logistic regression analysis was used to predict pulmonary hypertension. All significant variables on the univariate level were included in multivariate models, adjusted for age, gender, and residence. Regarding pulmonary parameters, PAAT was a significant predictor (OR = 1.05, 95% CI = 1.024 - 1.077, P < 0.001). Regarding RV diameters, proximal (OR = 9.109, 95% CI = 3.116 - 26.635, P < 0.001), distal (OR = 59.645, 95% CI = 10.077 - 353.035, P < 0.001), and peripheral (OR = 2.117, 95% CI = 1.296 - 3.459, P = 0.003) diameters were significant predictors. TAPSE was a significant predictor of pulmonary hypertension (OR = 2.214, 95% CI = 1.548 - 3.166, P < 0.001). Regarding E/A on RV, A wave (OR = 1.202, 95% CI = 1.109 - 1.303, P < 0.001) and E/A (OR = 0.002, 95% CI = 0 - 0.033, P < 0.001) were significant predictors. Regarding TDI on RV, MPI (OR = 9.924 X 10¹⁶, 95% CI = 4.380 X 10⁸ - 2.248 X 10²⁵, P < 0.001) was a significant predictor, in addition to S wave (OR = 1.365, 95% CI = 1.132 - 1.646, P = 0.001), A wave (OR = 1.393, 95% CI = 1.176 - 1.65, P < 0.001), and ET (OR = 0.981, 95% CI = 0.968 - 0.995, P = 0.007). Regarding IGFBP2, it was a significant predictor for pulmonary hypertension (OR = 1.039, 95% CI = 1.021 - 1.058, P < 0.001) (Table 4).

Discussion

PAH represents a grave pulmonary vascular disorder that frequently advances swiftly, leading to RV failure and ultimately death in the absence of intervention (17). While pediatric and adult forms of the disease share some similarities, there are notable differences in various epidemiological aspects, clinical manifestations, and the suitability of diagnostic approaches between these age groups (18).

In the present study, no significant differences were observed between the studied groups regarding age and sex similar to Yang et al. They found that there was no significant difference between the studied groups regarding the demographic (2).

The most frequent etiology for PH in our study was congenital heart defects, followed by left sided lesion and idiopathic mitral valve lesion, Upper air way diseases. In this regard, Lammers et al., reported that among the PHT cases most cases had idiopathic PHT followed by cases with associated PHT (19).

In the present study, regarding pulmonary parameters, Group A revealed significantly higher MPAP, and PAAT than group B.

In this study, Group A exhibited notably larger RV diameters in comparison to Group B. These findings align with those reported by Lammers et al., who also observed significant

differences in planimetric measurements of right and left atrial areas, pulmonary artery dimensions, tricuspid and mitral valve diameters, and diastolic right intraventricular diameter between PHT group and the control group. (19)

In our study, TAPSE, in Group A showed significantly lower TAPSE than Group B denoting systolic RV dysfunction.

Similar to Peter et al. reported that the median TAPSE was significantly lower in the PH group compared with the no PH group (20).

In our study, E/A on RV, Group A demonstrated a significantly higher A wave ($P < 0.001$) than Group B. In contrast, they demonstrated significantly lower E/A ($P < 0.001$). No significant differences were observed regarding E wave and DT ($P = 0.229$ and 0.132 , respectively).

PH cases in our study demonstrated significantly higher MPI ($P < 0.001$) in group A than group B. denoting systolic and diastolic dysfunction, Similar to Cabrita et al., Their study noted that MPI Doppler was significantly higher in pulmonary hypertension group than controls. (21).

In our study, Group A demonstrated significantly higher IGFBP2 than Group B. similar to Yang et al., and Griffiths et al., found that Serum IGFBP2 was elevated in PAH subjects compared to controls (22).

In our study, ROC analysis was done for IGFBP2, It revealed a significant excellent AUC of 0.923, with a 95% CI = 0.862 – 0.984 ($P < 0.001$). The best cutoff point was >168 , at which sensitivity and specificity were 95% and 77.5%, respectively. The positive and negative predictive values were 80.9% and 93.9%, respectively.

Consistent with our findings, Yang et al. illustrated that IGFBP2 exhibited the highest performance, yielding AUC of 0.76 ($P < 0.0001$). A discerning serum IGFBP2 threshold of 262.8 ng/ml was ascertained to delineate between individuals afflicted with PAH and those in the control group. This demarcation exhibited a sensitivity of 62.2% and specificity of 78.5% for PAH, accompanied by negative and positive predictive values of 79% and 84%, respectively (2).

In the present investigation, notable positive correlations were identified between IGFBP2 concentrations and both pulmonary artery pressure as well as the dimensions of the RV. Similar to Yang et al., reported that IGFBP2 correlated significantly with PAP (2).

In our study, IGFBP2 showed significant positive correlations with E wave. No significant correlations were reported with A wave.

Similar to Koh et al. (23).

In the present study, IGFBP2 showed significant positive correlations with MPI ($r = 0.619$, $P < 0.001$).

When correlated different variables for prediction of IGFBP2 it was found that : MPAP, PAAT, Basal, Mid RV, E wave, E/A MPI, and E wave were significant predictors for IGFBP2. When correlated different variables for prediction of pulmonary hypertension, it was found that

PAAT, RV diameters, TAPSE, A wave, MPI, S wave, A wave, ET, and IGFBP2 were significant predictors for pulmonary hypertension (24).

Conclusion

PHT was associated with elevation of pulmonary artery pressure, RV dilatation with RV systolic, and diastolic dysfunction. PHT cases had elevated levels of IGFBP2 which proved to be a good predictor of pulmonary hypertension with sensitivity and specificity were 95% and 77.5%, respectively. IGFBP showed significant correlation with severity of PH in terms of Pulmonary artery pressure and MPI of RV.

This study was limited by its single-center design, potentially limiting its generalizability. Additionally, the small sample size and lack of follow-up data on cases prevented a thorough assessment of IGFBP2's prognostic role in the disease.

References:

1. Sarah B, Ashrith G, Sandeep S. Evaluation, Diagnosis, and Classification of Pulmonary Hypertension. *Methodist Debakey Cardiovasc J.* 2021;17:86-91.
2. Yang J, Griffiths M, Nies MK, Brandal S, Damico R, Vaidya D, et al. Insulin-like growth factor binding protein-2: a new circulating indicator of pulmonary arterial hypertension severity and survival. *BMC Med.* 2020;18:268.
3. Crespo-Leiro MG, Metra M, Lund LH, Milicic D, Costanzo MR, Filippatos G, et al. Advanced heart failure: a position statement of the Heart Failure Association of the European Society of Cardiology. *European journal of heart failure.* 2018;20:1505-35.
4. LeRoith D, Holly JMP, Forbes BE. Insulin-like growth factors: Ligands, binding proteins, and receptors. *Mol Metab.* 2021;52:101245.
5. Abouzeid CM, Shah T, Johri A, Weinsaft JW, Kim J. Multimodality Imaging of the Right Ventricle. *Curr Treat Options Cardiovasc Med.* 2017;19:82.
6. Malakan Rad E, Amani S, Ilali HM, Sedaghat A, Zanjani KS, Moghadam EA, et al. Color tissue doppler imaging of tricuspid annular plane systolic and diastolic excursion in children: A comparison of normal, volume-overloaded and pressure overloaded right ventricles. *Echocardiography.* 2022;39:496-513.
7. Mowers K, Fullerton J, Hicks D, Singh G, Johnson M, Anwar S. 3D echocardiography provides highly accurate 3D printed models in congenital heart disease. *Pediatric Cardiology.* 2021;42:131-41.
8. Mueller-Graf F, Merz J, Bandorf T, Albus CF, Henkel M, Krukewitt L, et al. Correlation of Pulse Wave Transit Time with Pulmonary Artery Pressure in a Porcine Model of Pulmonary Hypertension. *Biomedicines.* 2021;9:1212.
9. Augustine DX, Coates-Bradshaw LD, Willis J, Harkness A, Ring L, Grapsa J, et al. Echocardiographic assessment of pulmonary hypertension: a guideline protocol from the British Society of Echocardiography. *Echo Res Pract.* 2018;5:G11-g24.
10. Parasuraman S, Walker S, Loudon BL, Gollop ND, Wilson AM, Lowery C, et al. Assessment of pulmonary artery pressure by echocardiography-A comprehensive review. *Int J Cardiol Heart Vasc.* 2016;12:45-51.
11. Levy PT, Patel MD, Groh G, Choudhry S, Murphy J, Holland MR, et al. Pulmonary Artery Acceleration Time Provides a Reliable Estimate of Invasive Pulmonary Hemodynamics in Children. *J Am Soc Echocardiogr.* 2016;29:1056-65.

12. Kim J, Srinivasan A, Seoane T, Di Franco A, Peskin CS, McQueen DM, et al. Echocardiographic Linear Dimensions for Assessment of Right Ventricular Chamber Volume as Demonstrated by Cardiac Magnetic Resonance. *J Am Soc Echocardiogr.* 2016;29:861-70.
13. Speiser U, Hirschberger M, Pilz G, Heer T, Sievers B, Strasser RH, et al. Tricuspid annular plane systolic excursion assessed using MRI for semi-quantification of right ventricular ejection fraction. *Br J Radiol.* 2012;85:e716-21.
14. Mottram PM, Marwick TH. Assessment of diastolic function: what the general cardiologist needs to know. *Heart.* 2005;91:681-95.
15. Correale M, Totaro A, Ieva R, Ferraretti A, Musaico F, Di Biase M. Tissue Doppler imaging in coronary artery diseases and heart failure. *Curr Cardiol Rev.* 2012;8:43-53.
16. Goroshi M, Chand D. Myocardial Performance Index (Tei Index): A simple tool to identify cardiac dysfunction in patients with diabetes mellitus. *Indian Heart J.* 2016;68:83-7.
17. Hester J, Ventetuolo C, Lahm T. Sex, gender, and sex hormones in pulmonary hypertension and right ventricular failure. *Comprehensive Physiology.* 2019;10:125.
18. Kabeerdoss J, Paliana RK, Karkhele R, Kumar TS, Danda D, Singh S. Severe COVID-19, multisystem inflammatory syndrome in children, and Kawasaki disease: immunological mechanisms, clinical manifestations and management. *Rheumatology international.* 2021;41:19-32.
19. Lammers AE, Haworth SG, Riley G, Maslin K, Diller G-P, Marek J. Value of Tissue Doppler Echocardiography in Children with Pulmonary Hypertension. *Journal of the American Society of Echocardiography.* 2016;25:504-10.
20. Peter ID, Asani MO, Abdullahi SU, Aliyu I, Obaro SK, Bode-Thomas F. Pulmonary hypertension and right ventricular function in Nigerian children with sickle cell anaemia. *Trans R Soc Trop Med Hyg.* 2019;113:489-96.
21. Zimbarra Cabrita I, Ruisanchez C, Dawson D, Grapsa J, North B, Howard LS, et al. Right ventricular function in patients with pulmonary hypertension; the value of myocardial performance index measured by tissue Doppler imaging. *Eur J Echocardiogr.* 2010;11:719-24.
22. Griffiths M, Yang J, Nies M, Vaidya D, Brandal S, Williams M, et al. Pediatric pulmonary hypertension: insulin-like growth factor-binding protein 2 is a novel marker associated with disease severity and survival. *Pediatric research.* 2020;88:850-6.
23. Koh HWL, Pilbrow AP, Tan SH, Zhao Q, Benke PI, Burla B, et al. An integrated signature of extracellular matrix proteins and a diastolic function imaging parameter predicts post-MI long-term outcomes. *Front Cardiovasc Med.* 2023;10:1123682.
24. Yang J, Griffiths M, Nies MK, Brandal S, Damico R, Vaidya D, et al. Insulin-like growth factor binding protein-2: a new circulating indicator of pulmonary arterial hypertension severity and survival. *BMC Medicine.* 2020;18:268.